Educational Administration: Theory and Practice
2024, 30(1), 5832-5839
ISSN: 2148-2403
https://kuey.net/

Research Article

Influence of Angle of Attack on the lift and drag characteristics of an aerofoil under turbulent conditions using Computational Fluid Dynamics (CFD) approach

Rushikesh Sonawane[1], Jay Rajkumar Meshram[1], Raja Sekhar Dondapati[1*]

[1*]School of Mechanical Engineering, Lovely Professional University, Phagwara, Punjab 144411, India

* **Corresponding Author:** Raja Sekhar Dondapati
*email: drsekhar@ieee.org, Ph: +91-8427474117

Citation: Raja Sekhar Dondapati et al (2024) Influence of Angle of Attack on the lift and drag characteristics of an aerofoil under turbulent conditions using Computational Fluid Dynamics (CFD) approach, *Educational Administration: Theory and Practice*, 30(1) 5832-5839,
Doi: 10.53555/kuey.v30i1.9266

ARTICLE INFO

ABSTRACT

In the process of energy saving in aviation industry without compromising on the performance, it is essential to reduce drag forces and increase the lift forces. Hence, the research is focused on designing the different airfoils. However, the fluid flow analysis over the designed airfoil is an important task in assessing the performance. As the experimental investigations are more expensive to perform at higher Reynolds Numbers, an alternative method using computational simulations is adapted in the present work. Computational Fluid Dynamics (CFD) plays an important role in the various engineering fields in providing the accurate solutions with higher order discretization methods. The various angle of attack of an aerofoil has a great impact on the aerodynamic performance. Therefore, the optimization of aerofoil by considering angle of attack is necessary. The distinctive aerofoil shape is characterized by a large leading-edge radius, condensed curvature over the middle region of the upper surface, and substantial aft camber. The present work emphasizes the computational study of flow separation over aerofoil NACA 63-412 at different angle of attack (0^0, 7^0, 09^0, 11^0, 13^0, 15^0) and different Reynolds numbers using CFD (Computational fluid dynamics) simulation. Parameters such as velocity, drag and lift coefficient at Reynolds numbers 2.79 $x10^6$, 4.60 $x10^6$, 6.13 $x10^6$, 7.66 $x10^6$ and 9.19 x 10^6 at various angle of attack ranging from 0^0 to 15^0 are studied in the present work. It is observed that lift coefficient is increase with increasing angle of attack up to 15^0 and the drag coefficient increases with increasing angle of attack upto 15^0.

Keywords: Computational fluid dynamics; Lift and Drag Coefficient; Angle of Attack; Reynolds number; Pressure; Velocity

1 Introduction

The science of fluid dynamics and its applications in various engineering domains have significantly shaped the modern world. From aviation to renewable energy, the understanding and manipulation of airflow around solid bodies have been pivotal in achieving remarkable advancements. Airfoils, also known as wings or blades, constitute an essential element in this intricate interplay of forces and fluids. Aerodynamics, that deals with interaction of air with the moving bodies, is the backbone of design of aircrafts, space shuttles etc. One of the primary parts of an aircraft that aerodynamics plays a vital role is its wings. The design and analysis of wings is often done to increase lift characteristics and decrease the drag characteristics as much as possible. Recently, few studies have been done on the symmetric aerofoil NACA 0012 and analysed the impact of various design modifications to enhance its lift-drag ratios [1]. They performed numerical simulation on the 2-D aerofoil and the results are compared to the standard data for validation. Further, an aerodynamic analysis of supercritical NACA sc (2)-0714 aerofoil has been performed using CFD. This work emphasizes the computational study of flow separation over Supercritical Aerofoil NACA SC (2)-0714 at different angle of attack using CFD (Computational fluid dynamics) simulation [2]. Parameters which are

observed are Pressure drag, Drag and Lift coefficient at Mach number 0.6. Moreover the investigation of NACA 63 and NACA 64 6-digit series of airfoils has been done in the NACA LTPT in view to verify the RFOIL calculated aerofoil characteristics for high Reynolds numbers [4]. The study has been done to analyze the effect of Reynolds Number on Aerodynamic Characteristics of an Aerofoil with Flap. It demonstrated the flow characteristics for designed aerofoil and it is shown graphically at solution steps along with lift and drag plot against angle of attack [5]. Furthermore, the study of evolution of the aerodynamic performance parameters and flow field of two dimensional airfoils called NACA 63-018 at different Reynolds numbers 3×10^6, 6×10^6 and 9×10^6 has been done with different angle of attack ranging from 0° to 16° [6]. The numerical investigation of the rotation speed and Reynolds number variations has been done on a NACA 0012 aerofoil. In this study, the hydrodynamic characteristics of a marine rudder with the NACA 0012 section are studied using computational fluid dynamics analyses in order to better understand the influence of rotational speed on the rudder and to determine its relationship with the Reynolds number. Commercial software ANSYS Fluent is used to perform RANS simulations for the investigation [7]. Also, the analysis is carried out for a free stream Reynolds number of 6 million for which the wind tunnel results are available. This CFD analysis is carried out on NACA 23024 aerofoil using ANSYS Fluent Solver [8]. In addition to that the study on the analysis of NACA 0020 aerofoil profile rotor blade has been conducted using CFD approach [9]. Also, the comparative analysis of low velocity vertical axis wind turbine NACA blades at different attacking angle of attack has been completed using CFD approach [10]. The objective of this study is to understand the phenomena of the uniqueness of aerofoil shape. The present study focuses on the influence of angle of attack on the lift and drag characteristics of aerofoil using Computational Fluid Dynamics (CFD) approach. The computational study of flow separation over aerofoil NACA 63-412 at different angle of attack (0°, 7°, 09°, 11°, 13°, 15°) and different Reynolds numbers using CFD (Computational fluid dynamics) simulation is conducted. Parameters which we will be observing are pressure contour, velocity contour, velocity vectors, drag and lift coefficient at Reynolds numbers 2.79 x10^6, 4.60 x10^6, 6.13 x10^6, 7.66 x10^6 and 9.19 x10^6 at various angle of attack ranging from 0° to 15°. By doing this study we will come to know how the various inlet velocities as well as the angle of attack affect the lift and drag characteristics of the airfoil. Changes in pressure and velocity of air due to the distinct shape of aerofoil at various inlet conditions will also be observed during this work. This work can be helpful to determine the lift and drag characteristics of NACA 63-412 aerofoil and its behavior under various inlet conditions.

2 METHODOLOGY AND CFD ANALYSIS

The present work focuses on the investigation of lift and drag forces of NACA 63-412 aerofoil. The coordinates describing the aerofoil were obtained from the NACA database which described the aerofoil by 51 points. The NACA 63-412 aerofoil has a maximum thickness of 12% at 34.9% chord and a maximum camber of 2.2% at 50% chord. In number 63-412 in NACA 63-412 , the number 6 denotes the series designation, the number 3 denotes the minimum pressure occurs at 0.3 chord from leading edge, number 4 denotes the design lift coefficient is 0.4, and the aerofoil is 12% thick of chord. The Modeled Profile of NACA 63-412 is shown in Figure 1a) and the corresponding meshed part is shown in Figure 1b). The boundary conditions considered for the present analysis are shown in Figure 1c). The domain was discretized by a structured grid of quadrilaterals with 177708 nodes and 176900 elements.

2.1 Governing equations

To solve this problem numerically following equation are used by FLUENT CFD software.
The time-averaged conservation of mass (continuity equation) for 3-D flow can be written as:

$$\frac{\partial \overline{u}}{\partial x}+\frac{\partial \overline{v}}{\partial y}+\frac{\partial \overline{w}}{\partial z}=0 \quad (1)$$

where, $\overline{u}$, $\overline{v}$ and $\overline{w}$ are known as time-averaged velocity components in x, y and z directions respectively.
The time-averaged conservation of momentum equations for 3-D flow are as follows:
X-momentum

$$\rho\left(\frac{\partial \overline{u}}{\partial t}+\overline{u}\frac{\partial \overline{u}}{\partial x}+\overline{v}\frac{\partial \overline{u}}{\partial y}+\overline{w}\frac{\partial \overline{u}}{\partial z}\right)=F_X-\frac{\partial \overline{p}}{\partial x}+\mu\nabla^2\overline{u}-\rho\left(\frac{\partial \overline{u'u'}}{\partial x}+\frac{\partial \overline{u'v'}}{\partial y}+\frac{\partial \overline{u'w'}}{\partial z}\right) \quad (2)$$

Y-momentum

$$\rho\left(\frac{\partial \overline{v}}{\partial t}+\overline{u}\frac{\partial \overline{v}}{\partial x}+\overline{v}\frac{\partial \overline{v}}{\partial y}+\overline{w}\frac{\partial \overline{v}}{\partial z}\right)=F_Y-\frac{\partial \overline{p}}{\partial y}+\mu\nabla^2\overline{v}-\rho\left(\frac{\partial \overline{u'v'}}{\partial x}+\frac{\partial \overline{v'v'}}{\partial y}+\frac{\partial \overline{w'v'}}{\partial z}\right) \quad (3)$$

Z-momentum

$$\rho\left(\frac{\partial \overline{w}}{\partial t}+\overline{u}\frac{\partial \overline{w}}{\partial x}+\overline{v}\frac{\partial \overline{w}}{\partial y}+\overline{w}\frac{\partial \overline{w}}{\partial z}\right)=F_z-\frac{\partial \overline{p}}{\partial z}+\mu\nabla^2\overline{w}-\rho\left(\frac{\partial \overline{u'w'}}{\partial x}+\frac{\partial \overline{v'w'}}{\partial y}+\frac{\partial \overline{w'w'}}{\partial z}\right) \quad (4)$$

where, $\nabla^2\overline{u}=\left(\frac{\partial^2\overline{u}}{\partial x^2}+\frac{\partial^2\overline{u}}{\partial y^2}+\frac{\partial^2\overline{u}}{\partial z^2}\right)$, $\nabla^2\overline{v}=\left(\frac{\partial^2\overline{v}}{\partial x^2}+\frac{\partial^2\overline{v}}{\partial y^2}+\frac{\partial^2\overline{v}}{\partial z^2}\right)$, $\nabla^2\overline{w}=\left(\frac{\partial^2\overline{w}}{\partial x^2}+\frac{\partial^2\overline{w}}{\partial y^2}+\frac{\partial^2\overline{w}}{\partial z^2}\right)$
The generalized time–averaged momentum equation for all three directions in tensor form can be written as

$$\rho\frac{D\overline{u}_i}{Dt}=F_i-\frac{\partial \overline{p}}{\partial x_i}+\mu\nabla\overline{u}_i-\rho\left(\frac{\partial \overline{u_i'u_j'}}{\partial x_j}\right) \quad (5)$$

i and j are the normal components of tensor taking a value of Zero if i≠j and one if i=j, $\rho\left(\frac{\partial\overline{u_i'u_j'}}{\partial x_j}\right)$ is characterized as Reynolds stress or turbulent shear stress and $\left(\mu\frac{\partial u_i}{\partial x_j}-\rho\overline{u_i'u_j'}\right)$ is known as total shear stress τ_{ij}. u represent the instantaneous velocity component, and u' is known as fluctuating velocity component. F_x, F_y and F_z are known as body forces and neglected for the present simulations.
The time-averaged energy equations for 3-D flow are as follows:

$$\rho C_P\left[\overline{u}\frac{\partial\overline{T}}{\partial x}+\overline{v}\frac{\partial\overline{T}}{\partial y}+\overline{v}\frac{\partial\overline{T}}{\partial z}\right]=\frac{\partial}{\partial x}\left[k\frac{\partial T}{\partial x}-\rho C_P\overline{u'T'}\right]+\frac{\partial}{\partial y}\left[k\frac{\partial T}{\partial y}-\rho C_P\overline{v'T'}\right]+\frac{\partial}{\partial z}\left[k\frac{\partial T}{\partial z}-\rho C_P\overline{w'T'}\right] \quad (6)$$

Turbulence modelling:
The shear-stress transport (SST) $k-\omega$ model was adopted for this simulation.

$$\frac{\partial(\rho k)}{\partial t}+\frac{\partial(\rho k u_i)}{\partial x_i}=\frac{\partial}{\partial x_j}\left(\Gamma_k\frac{\partial k}{\partial x_j}\right)+\widetilde{G_k}-Y_k+S_k \quad (7)$$

and

$$\frac{\partial(\rho\omega)}{\partial t}+\frac{\partial(\rho\omega u_j)}{\partial x_j}=\frac{\partial}{\partial x_j}\left(\Gamma_\omega\frac{\partial\omega}{\partial x_j}\right)+\widetilde{G_\omega}-Y_\omega+D_\omega+S_\omega \quad (8)$$

In these equations $\widetilde{G_k}$ represents the generation of turbulence kinetic energy due to mean velocity gradients, G_ω represents the generation of ω, calculated as described for the standard $k-\omega$ model in Modelling in the Turbulence Production [11]. Γ_k *and* Γ_ω are represent the effective diffusivity of k *and* ω, respectively. Y_k *and* Y_ω represent the dissipation of k *and* ω due to turbulence. D_ω represents the cross-diffusion term. S_k *and* S_ω are user-defined source terms[11]. For closure of the problem an extra ideal gas equation is considered in order to capture compressible flow effects given by

$$PV=n\bar{R}T \quad (9)$$

Where P=pressure (Pa), V= volume (m^3), n= no. of moles, $\bar{R}$= Universal gas constant (J/mol K) and T= Absolute temperature (K). Effect of Reynolds Number on Aerodynamic Characteristics of an Aerofoil is given by following empirical relation.

$$Re=\frac{\rho v l}{\mu} \quad (10)$$

Analysis on the aerofoil profile is carried out to find the values of C_D and C_L at different values of angle of attack at different Reynolds number of 2.79 x10^6, 4.60 x10^6, 6.13 x10^6, 7.66 x10^6 and 9.19 x10^6. The velocity components are calculated for each angle of attack case.

Table 1 shows some of the cases considered for the present analysis. The flow inlet velocities were taken as 45.6 m/sec, 75, 100 m/sec, 125 m/sec and 150 m/sec in order to match the required Reynolds number 2.79 x10^{-6}, 4.60 x10^{-6}, 6.13 x10^{-6}, 7.66 x10^{-6} and 9.19 x10^{-6} respectively.

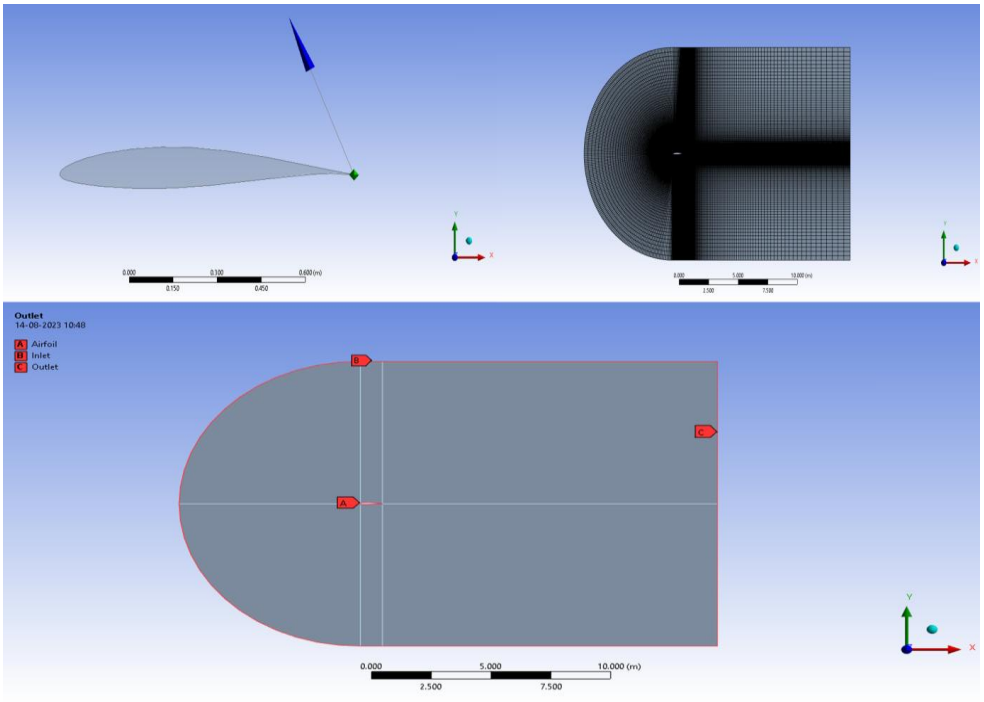

Figure 1 a) Aerofoil profile created using Design modeller b) Complete meshing of a body c) Boundary Conditions

Table 1 Inlet velocities for various cases

Cases	Reynolds number [Re]	Inlet velocity [m/s]	AOA [deg.]
Case 1	2.79 x10^6	45.6	0
			7
			9
			11
			13
			15
Case 2	4.60 x10^6	75	0
			7
			9
			11
			13
			15
Case 3	6.13 x10^6	100	0
			7
			9
			11
			13
			15
Case 4	7.66 x10^6	125	0
			7
			9
			11
			13
			15
Case 5	9.19 x10^6	150	0
			7
			9
			11
			13
			15

3 RESULTS AND DISCUSSION

Drag and lift coefficients

A numerical investigation on NACA 63-412 for various angles of attack at different Reynolds number is done. The model was solved with a range of different angles of attack from 0° to 15° at different Reynolds number. Drag coefficient and Lift coefficients were plotted against various Reynolds Numbers and Angle of Attacks. For each case, the C_d and C_l have been calculated.

Figure 2 shows the C_d values obtained from simulations conducted for various AOA for various Re numbers. Similarly, Figure 3 shows the C_l values obtained from simulations conducted for various AOA for various Re numbers. Figure 2 shows the effect of AOA on drag Coefficient. Figure 3 shows the effect of AOA on lift Coefficient. Figure 4 shows the effect of Reynolds number on drag Coefficient. While, Figure 5 shows the effect of Reynolds number on lift Coefficient. It is also observed that the drag coefficient increasing with increasing lift coefficient. It is also a function of angle of attack. There was small variation in drag coefficient at angle of attack 0°-9° at higher angle of attack transition to turbulent flow occurs over the aerofoil surface causing sharp increase in drag coefficient. It could be observed that the drag coefficient is decreasing with increasing Reynolds number. This is because of the drag on any aerodynamic body is composed of pressure drag and skin friction drag. The basic source of aerodynamic force on a body is the pressure and shear stress distribution on the body surface. The division of total drag on to its components of pressure and skin friction drag is frequently useful in analyzing aerodynamic phenomena. The NACA 63-412 air foil is a stream lined body. The most of the drag of the stream lined body is due to skin friction. Skin friction coefficient is a function of Reynolds number. It is inversely proportional to the Reynolds number so, drag coefficient decreases as Reynolds number increases. It can be observed that the lift coefficient is increasing with increasing Reynolds number at each angle of attack up to 15°. Maximum lift coefficient is dependent upon Reynolds number. This makes sense, because maximum lift coefficient is governed by viscous effects, and

Reynolds number is a similarity parameter that governs the strength of inertia forces relative to viscous forces in the flow.

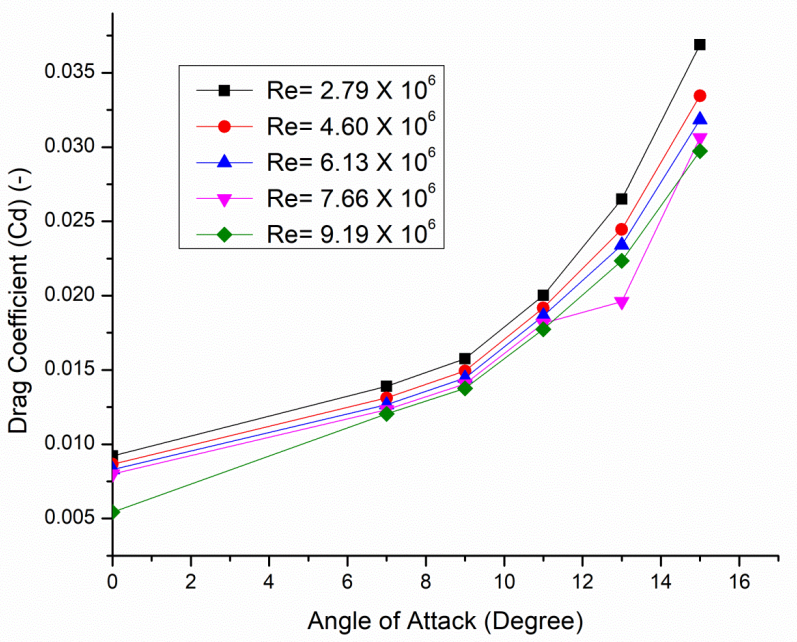

Figure 2 Effect of AOA on drag Coefficient

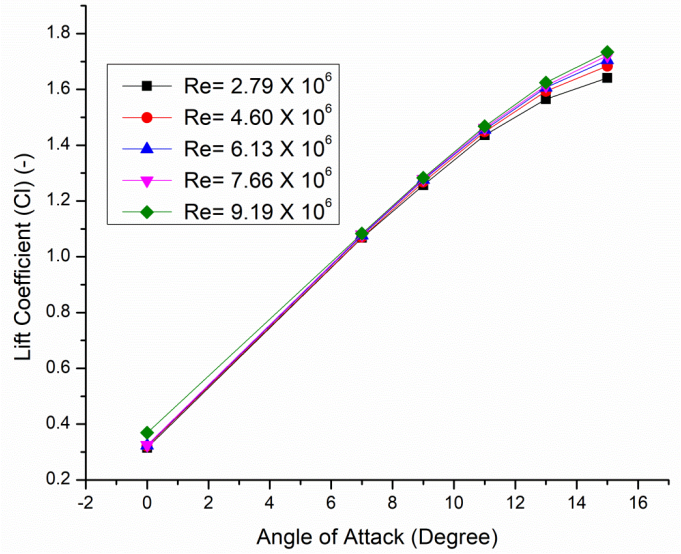

Figure 3 Effect of AOA on lift Coefficient

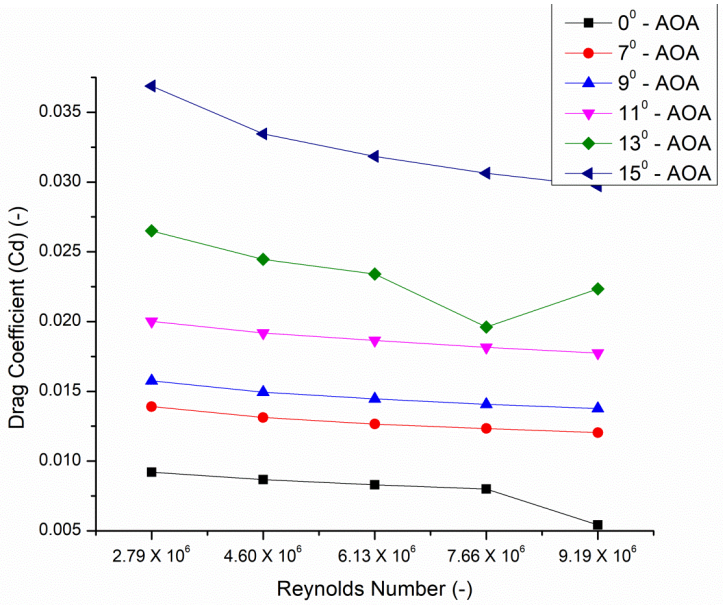

Figure 4 Effect of Reynolds number on drag Coefficient

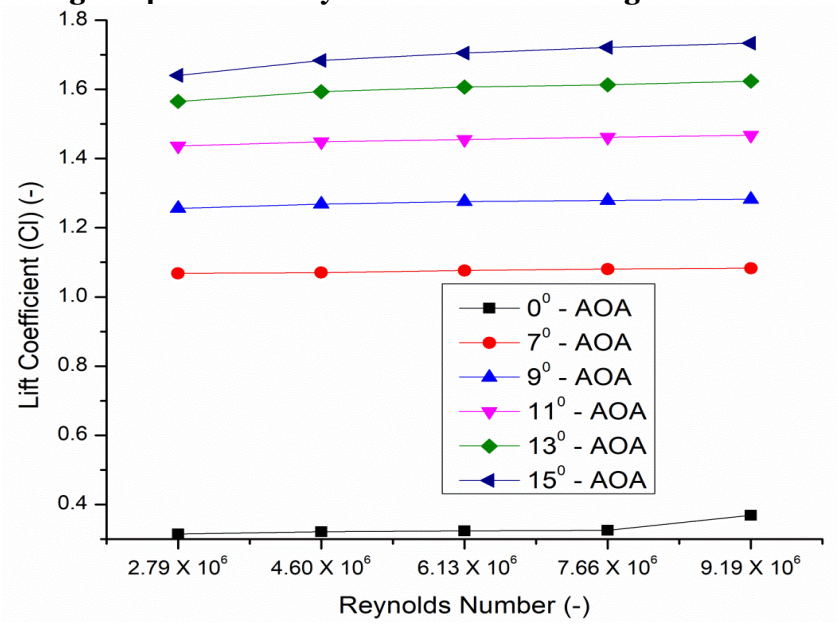

Figure 5 Effect of Reynolds number on lift Coefficient

Velocity distribution

The effect of air velocity on the pressure distribution around an aerofoil (a streamlined shape designed to generate lift when air flows over it) is an important factor in understanding aerodynamics and lift generation. As air flows over an aerofoil, its velocity and pressure distributions play a significant role in determining lift, drag, and overall aerodynamic performance. When the air accelerates over the curved upper surface of the aerofoil, the kinetic energy (velocity) increases causing a reduction in pressure. This can show the effect of air velocity on airfoil shape for different angles of attack and Reynolds number (Figure 6). It can be seen that the there is a region of low velocity and high pressure at the leading edge (stagnation point) and region of low pressure and high velocity on the upper surface of aerofoil. This lower pressure region above the aerofoil contributes to the generation of lift. The aerofoil's shape and curvature also lead to a velocity gradient along its surface.

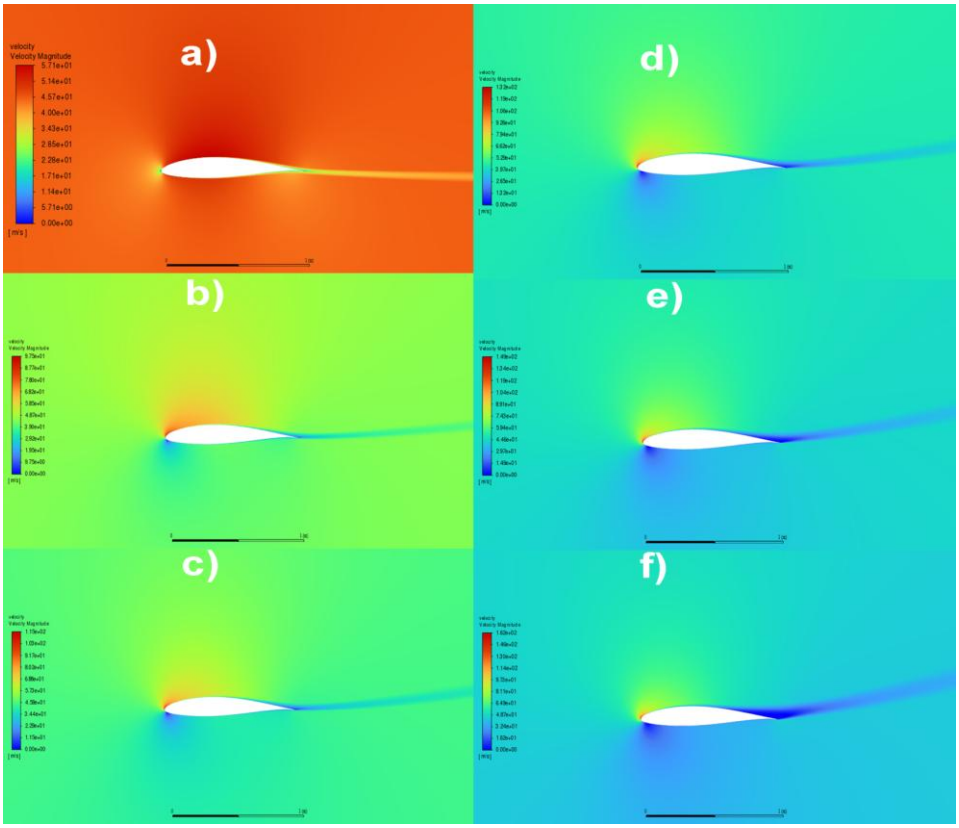

Figure 6 Velocity magnitude contours at angle of attack 0° to 15° at a Reynolds number of 2.79 x10⁶

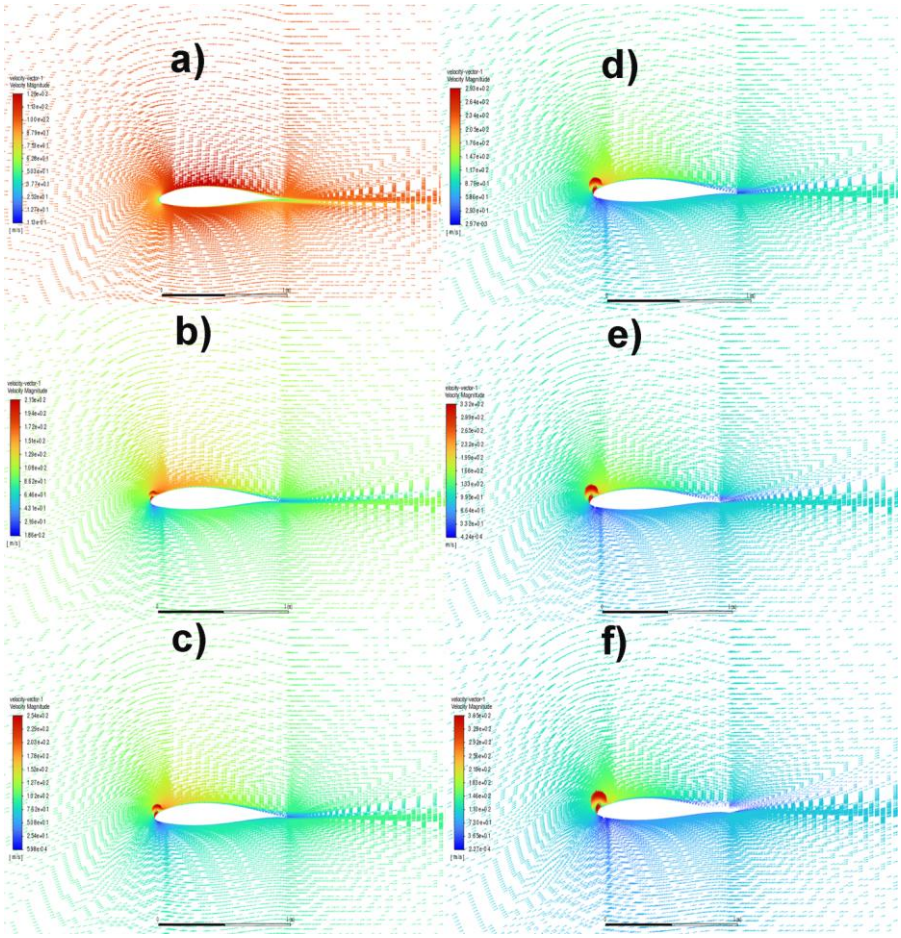

Figure 7 Velocity vector contours at angle of attack 0° to 15° at a Reynolds number of 4.60 x10⁶

The airflow near the leading edge is relatively slow compared to the upper surface, resulting in a higher pressure region on the lower surface. This pressure difference between the upper and lower surfaces contributes to the lift generation. If the air velocity becomes too high, it can lead to flow separation and a stall. A stall occurs when the airflow over the upper surface of the aerofoil becomes turbulent and detached, causing a significant reduction in lift and an increase in drag. Stall can be influenced by factors such as angle of attack, aerofoil shape, and Reynolds number (which consider the aerofoil's size and velocity relative to its viscosity) (Figure 7).

4 CONCLUSIONS

It can be concluded from the present CFD analysis that the angle of attack and air velocity are some of the key parameters one must concentrate in order to understand the concept of lift and drag characteristics of an aerofoil. It can also be concluded that the angle of attack, air velocity and the profile of an aerofoil is responsible to generate a low-pressure region over the aerofoil and as a result the lift force. Hence, it may be desirable to keep this fact in view while choosing the aerofoil of optimum characteristics. This CFD analysis concluded that the lift coefficient and Drag coefficient are the function of angle of attack. The lift coefficient is increase with increasing angle of attack up to 15° and the drag coefficient increases with increasing angle of attack upto 15°. The maximum value of lift coefficient is found to be 1.7338 at AOA 15° with Reynolds number of 9.19 x 10^6. Similarly, the value of drag coefficient is found to be 0.036884 at AOA 15° with Reynolds number of 2.79 x 10^6.

REFERENCES

[1] T. Srinivasa Rao, T. Mahapatra, and S. Chaitanya Mangavelli, “Enhancement of Lift-Drag characteristics of NACA 0012,” Mater Today Proc, vol. 5, no. 2, Part 1, pp. 5328–5337, 2018, doi: https://doi.org/10.1016/j.matpr.2017.12.117.

[2] Ravikumar and Dr. S B Prakash, “AERODYNAMIC ANALYSIS OF SUPERCRITICAL NACA SC (2)-0714 AIRFOIL USING CFD,” International Journal of Advanced Technology in Engineering and Science, vol. 2, no. 7, pp. 285–293, Jul. 2014.

[3] H. H. , Jr. Hurt, Aerodynamics for Naval Aviators. Washington, D.C: DIRECTION OF COMMANDER, NAVAL AIR SYSTEMS COMMAND, 1965.

[4] W. Timmer, “An Overview of NACA 6-Digit Airfoil Series Characteristics with Reference to Airfoils for Large Wind Turbine Blades,” in 47th AIAA Aerospace Sciences Meeting including The New Horizons Forum and Aerospace Exposition, in Aerospace Sciences Meetings. American Institute of Aeronautics and Astronautics, 2009. doi: doi:10.2514/6.2009-268.

[5] Md. Hasanuzzaman and Mohammad Mashud, “Effect of Reynolds Number on Aerodynamic Characteristics of an Airfoil with Flap,” Annals of Pure and Applied Mathematics, vol. 3, no. 1, pp. 27–40, May 2013.

[6] Abdul Azeez VP and John paul., “CFD Analysis of NACA 63-018 Airfoil at Different Reynolds-Number,” International Journal of Engineering Trends and Technology (IJETT), vol. 12, no. 5, pp. 258–264, Jun. 2014.

[7] M. Z. Sener and E. Aksu, “The numerical investigation of the rotation speed and Reynolds number variations of a NACA 0012 airfoil,” Ocean Engineering, vol. 249, p. 110899, 2022, doi: https://doi.org/10.1016/j.oceaneng.2022.110899.

[8] B. S. Anil Kumar, Ramalingaiah, S. Manjunath, and R. Ganganna, “Computational Investigation of Flow Separation over NACA 23024 Airfoil at 6 Million Free Stream Reynolds Number Using k-Epsilon Turbulence Model,” Mater Today Proc, vol. 5, no. 5, Part 2, pp. 12632–12640, 2018, doi: https://doi.org/10.1016/j.matpr.2018.02.246.

[9] S. Irfan Sadaq, S. Nawazish Mehdi, S. Danish Mehdi, and S. Yasear, “Analysis of NACA 0020 aerofoil profile rotor blade using CFD approach,” Mater Today Proc, vol. 64, pp. 147–160, 2022, doi: https://doi.org/10.1016/j.matpr.2022.04.205.

[10] M. Hasham Ali, S. Nawazish Mehdi, and M. T. Naik, “Comparative analysis of low velocity vertical axis wind turbine NACA blades at different attacking angles in CFD,” Mater Today Proc, vol. 80, pp. 2091–2100, 2023, doi: https://doi.org/10.1016/j.matpr.2021.06.119.

[11] *ANSYS-Fluent Theory Guide*. Canonsburg, PA: Ansys Inc, 2013.